Journal of Applied Polymer Science

Affinity-tuned peroxidase-like activity of hydrogel-supported Fe_3O_4 nanozyme through alteration of crosslinking concentration

Jilong Sang, Ronglan Wu, Pingping Guo, Juan Du, Shimei Xu, Jide Wang
Key Laboratory of Oil and Gas Fine Chemicals, Ministry of Education and Xinjiang Uyghur Autonomous Region, College of Chemistry and Chemical Engineering, Xinjiang University, Urumqi, Xinjiang, 830046, People's Republic of China
Correspondence to: S. Xu (E-mail: xushmei@hotmail.com)

ABSTRACT: In this work, we evaluated the effect of crosslinking concentration on the affinity of poly (2-acrylamido-2-methyl-1-propansulfonic acid) (PAMPS) hydrogel-supported Fe_3O_4 nanozyme towards substrates (tetramethylbenzidine (TMB) and H_2O_2). The peroxidase-like catalytic activity of PAMPS/Fe_3O_4 nanozyme was discussed with respect to crosslinking concentration of PAMPS hydrogel for the oxidation of TMB in the presence of H_2O_2 at room temperature. High catalytic activity was achieved due to good dispersion of Fe_3O_4 nanozyme in the hydrogel network and strong affinity of PAMPS hydrogel-supported Fe_3O_4 nanozyme towards substrates. The affinity between the hydrogel-supported Fe_3O_4 nanozyme and substrates can be improved by regulating the crosslinking concentration of PAMPS hydrogel without other trenchant experimental conditions. In addition, the result indicated that H_2O_2 can be detected even at a concentration as low as 1.5×10^{-6} mol L^{-1} with a linear detection range of 1.5–9.8 $\times 10^{-6}$ mol L^{-1}. Such investigations not only showed a new approach to improve the affinity and peroxidase-like activity of Fe_3O_4 nanozyme, but also verified its potential application in bio-detection and environmental chemistry. © 2015 Wiley Periodicals, Inc. J. Appl. Polym. Sci. **2016**, *133*, 43065.

KEYWORDS: biomimetic; catalysts; composites; crosslinking; kinetics

Received 6 September 2015; accepted 15 October 2015
DOI: 10.1002/app.43065

INTRODUCTION

In the past few decades, natural enzymes have been widely investigated and broadly applied in biomedical and catalytic applications due to their high catalytic efficiency and selectivity under mild conditions. However, most natural enzymes are not stable and demonstrate an inherently low durability to harsh reaction conditions. In addition, high costs of preparation, purification, and rigorous storage also restrict their pervasive applications. Meanwhile, their catalytic activity can be easily affected by environmental conditions.[1–3] As a result, enzyme immobilization techniques and artificial enzyme mimetics have been investigated to overcome the drawbacks.[4,5]

Nanozyme is a mimetic enzyme, which possesses both unique properties of nanomaterials and catalytic function of enzymes. The nanozymes have advantages of high stability and low cost when compared with natural enzymes.[6–8] Gao *et al.* first proved that Fe_3O_4 nanozyme exhibited an intrinsic enzyme mimetic activity similar to natural peroxides such as horseradish peroxidase (HRP), which opened the first case for the development of nanozyme in the biochemical field.[9] Fe_3O_4 nanozyme has exhibited fascinating prospects principally in biomedical and environmental applications including H_2O_2 and glucose detection,[10–13] and wastewater treatment.[14,15] It was reported that the peroxidase-like activity depended heavily on dispersion and content of Fe_3O_4 nanozyme,[16–19] as well as affinity towards substrates.[20] Among the researches, affinity was usually improved by modifying the surface of Fe_3O_4 nanoparticles with small molecules or linear polymers.[11] In contrast, hydrogels, as a kind of three-dimensional (3D) network polymer, can provide a specific microenvironment for the *in situ* synthesis of inorganic nanoparticles. Furthermore, the hydrogels can act as nanoreactors for catalytic reaction of nanozyme.[21,22] Poly(2-acrylamido-2-methyl-propane sulfonic acid sodium salt) (PNaAMPS) hydrogel was first reported to tune size and shape of Fe_3O_4 nanoparticles by adjusting the crosslinking concentration of the hydrogel.[23] The PNaAMPS hydrogel-supported Fe_3O_4 nanoparticles exhibited excellent catalytic activity and provided a sensitive response toward H_2O_2 detection. However, it still remains unknown about the affinity of hydrogel-supported Fe_3O_4 enzyme towards substrate. Besides, dispersion problem may still existed if loading of Fe_3O_4 enzyme was driven by strong electrostatic attraction between negatively charged functional groups of hydrogels and positively charged iron ions.

In this work, we evaluated the effect of crosslinking concentration on the affinity of poly(2-acrylamido-2-methyl-1-propansulfonic acid) (PAMPS) hydrogel-supported Fe_3O_4 nanozyme towards substrates [tetramethylbenzidine (TMB) and H_2O_2]. Besides, different from the previous report, AMPS was chosen instead of NaAMPS in attempt to avoid aggregation of Fe_3O_4 nanoparticles caused by strong electrostatic attraction and simplify the evaluation process of Fe_3O_4 loading. We found that the affinity depended on the content of the Fe_3O_4 nanozyme within hydrogel matrices and network size, which was adjusted by the different crosslinking concentration of the hydrogel. In addition, this is the first report in which the affinity between hydrogel-supported Fe_3O_4 nanozyme and substrates was tunable just by regulating the crosslinking concentration of the hydrogel without other trenchant experimental conditions. Moreover, PAMPS hydrogel-supported Fe_3O_4 nanozyme showed high peroxidase-like activity and H_2O_2 detection concentration was three times lower than the one in the case of PNaAMPS hydrogel-supported Fe_3O_4 nanoparticles.[23] In addition, the mimic enzyme can be recovered easily with an external magnet after the reaction completed.

EXPERIMENTAL

Materials

2-acrylamido-2-methyl-1-propansulfonic acid (AMPS) as monomer was purchased from Hansi chemicals, China. *N,N′*-methylenebisacrylamide (MBA) as a crosslinking agent, ammonium persulfate (APS) as an initiator, ferric chloride hexahydrate ($FeCl_3 \cdot 6H_2O$), and ferrous chloride tetrahydrate ($FeCl_2 \cdot 4H_2O$) were used as iron sources, were obtained from Shengao and Beichen Fangzheng, China, respectively. *N,N,N′,N′*-tetramethylenediamine (TEMED) as an accelerator, were obtained from Aldrich chemicals. Dimethyl sulfoxide (DMSO) as solvent, sodium acetate anhydrous and acetic acid glacial as buffer solution, and ammonia (25 wt %) as a reductant, were supplied by Zhiyuan chemicals, China. TMB and hydrogen peroxide (30 wt %) were applied for the catalytic studies, were obtained from Aldrich chemicals and Zhiyuan chemicals, China, respectively. All chemical reagents were of analytical grade. Deionized water was used for hydrogel preparation and the catalytic experiment.

Synthesis of PAMPS Hydrogels

PAMPS hydrogels with different crosslinking concentrations was prepared via free radical polymerization. Typically, 4.5 g of AMPS was dissolved in 4 mL deionized water to obtain transparent colorless solution under magnetic stirring. Then 1.7 mL 1.0 wt % of MBA was added to the above solution followed by 1 mL 5 wt % of APS and 100 μL of TEMED. After stirring for 5 min, the mix solution was placed at ambient temperature for 24 h to ensure thorough crosslinking polymerization. After gelation, the PAMPS hydrogels (1.0 wt %) were cut into small pieces and was washed with large quantities of deionized water to remove unreacted reagents. And the PAMPS hydrogel with other different concentrations of the crosslinking agent (1.5 or 0.5 wt %) were synthesized by the same procedure except for 1.5 wt % of MBA or 0.5 wt % of MBA instead of 1.0 wt % of MBA.

Fabrication of Fe_3O_4 Nanozyme in PAMPS Hydrogel (PAMPS/Fe_3O_4 Nanozyme)

Fe_3O_4 nanozyme within a PAMPS hydrogel network was fabricated by a co-precipitation reaction of $FeCl_2 \cdot 4H_2O$ and $FeCl_3 \cdot 6H_2O$ in the presence of ammonium hydroxide (25 wt %). In short, 7.3 g as-prepared PAMPS hydrogel with the concentrations of the crosslinking agent (1.5, 1.0, and 0.5 wt %) was swollen to reach equilibrium, then swollen PAMPS hydrogels were immersed in 15 mL (0.102 mol L^{-1}) aqueous solution of $FeCl_2 \cdot 4H_2O$ and $FeCl_3 \cdot 6H_2O$ (molar ratio of 1:2) for 48 h at ambient temperature. Subsequently, the iron ion loaded hydrogels, after washing with ionized water, immediately transferred into 200 mL an ammonia (25 wt %) aqueous solution and kept for 48 h at ambient temperature to form Fe_3O_4 nanoparticles in PAMPS hydrogels. The resultant PAMPS/Fe_3O_4 nanozyme was washed with deionized water and oven-dried to a constant weight at 60°C. The dry PAMPS/Fe_3O_4 nanozyme was ground to 80–100 meshes and kept in sealed plastic tube before use.

Characterization

The size and morphology of the PAMPS/Fe_3O_4 nanozyme were characterized by transmission electronic microscopy (TEM, Hitachi H-600) under vacuum operating at an acceleration voltage of 100 kV. Scanning electron microscopy (SEM) images of the PAMPS/Fe_3O_4 nanozyme were recorded with scanning electron microscopy (LEO-1430VP) with an accelerating voltage of 20 kV. Prior to observation, the composites were freeze-dried (FD-1-50) for 36 h, and sprayed with gold. To estimate the amounts of Fe_3O_4 nanozyme loadings and inspect the thermal stability of the compositions, thermogravimetric analysis (TGA, SDTQ600) was performed by heating samples from room temperature to 1000°C with a heating rate of 10°C/min under nitrogen atmosphere (flow rate, 10 mL/min). To ensure the accuracy of the iron content of the PAMPS/Fe_3O_4 nanozyme, nitrogen was chosen to protect the iron from being oxidized. The technique has been previously recorded for valuing the Fe_3O_4 nanozyme content of magnetic polymer particles.[24] The content of Fe_3O_4 nanozyme in the hydrogel can be calculated as in eq. (1)[25]:

$$\frac{Rq}{\Delta Wq} \times \Delta Wm + M = R \quad (1)$$

where R_q is the residue (wt %) at 1000°C of the bare hydrogel; $\triangle W_q$ and $\triangle W_m$ are the weight-loss percentages for bare hydrogel and nanocomposite hydrogel, which is between the initial and ending decomposition temperature, respectively; M is the weight percentage of Fe_3O_4 nanozyme in the hydrogel; and R is the residue at 1000°C (in wt %) for the hybrid hydrogel.

Fourier transform infrared spectroscopy (FTIR) of the composites were measured on an infrared spectrometer. Ultraviolet–visible (UV–vis) absorption spectra were conducted on an UV–VIS spectrophotometer (TU-1810). Magnetic measurements were investigated using a MicroSence EV9 vibrating sample magnetometer (VSM) at room temperature. The crystallographic properties and structure of the complex were acquired using an X-ray diffractometer (XRD) with Cu K_α radiation ($\lambda = 1.54178$ Å) in the range of 10 – 80°.

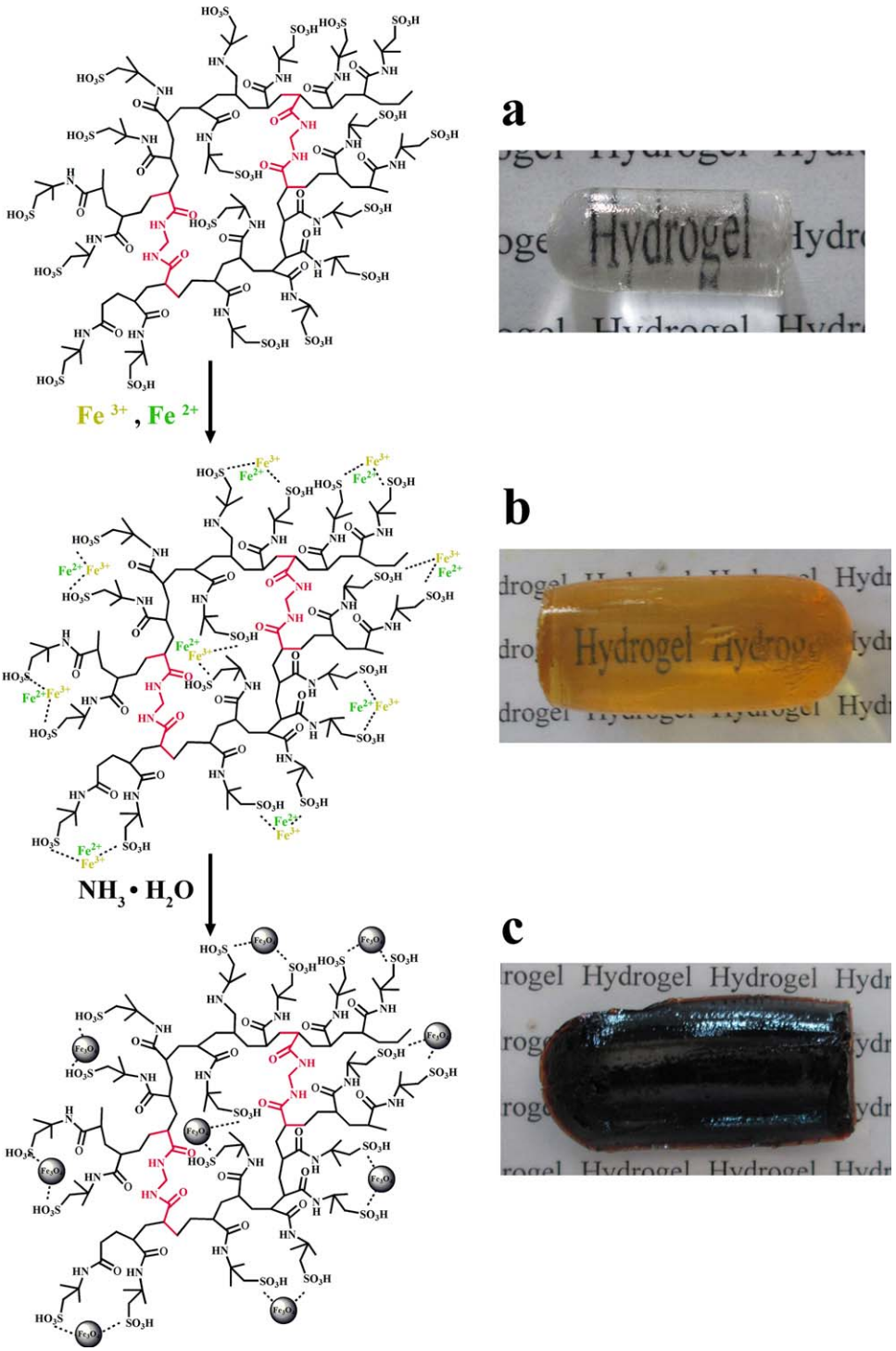

Figure 1. Preparation scheme of PAMPS/Fe_3O_4 nanozyme and its digital camera images (a) PAMPS hydrogel, (b) Fe (II) and Fe (III) ion-absorbed PAMPS hydrogel, and (c) Fe_3O_4 nanozyme in PAMPS hydrogel matrices. [Color figure can be viewed in the online issue, which is available at wileyonlinelibrary.com.]

Catalytic Experiments and Steady-State Kinetic Analysis

In order to investigate the catalytic activity of the PAMPS/Fe_3O_4 nanozyme: the typical catalytic reaction was carried out in sodium acetate anhydrous and acetic acid glacial buffer (6 mL, pH = 4) with PAMPS/Fe_3O_4 nanozyme (0.025 g), 0.098 mmol L^{-1}, H_2O_2 (2 μL, 1 wt %), and 0.55 mmol L^{-1} TMB (80 μL, 10 mg/mL in DMSO) at ambient temperature for 30 min. The steady-state kinetic analysis of PAMPS/Fe_3O_4 nanozyme with TMB as the substrate was performed by varying different concentrations (0.14, 0.28, 0.41, 0.55, and 0.68 mmol L^{-1}, respectively) of TMB at a fixed H_2O_2 concentration of 0.098 mmol L^{-1}. With H_2O_2 as the substrate, concentrations of H_2O_2

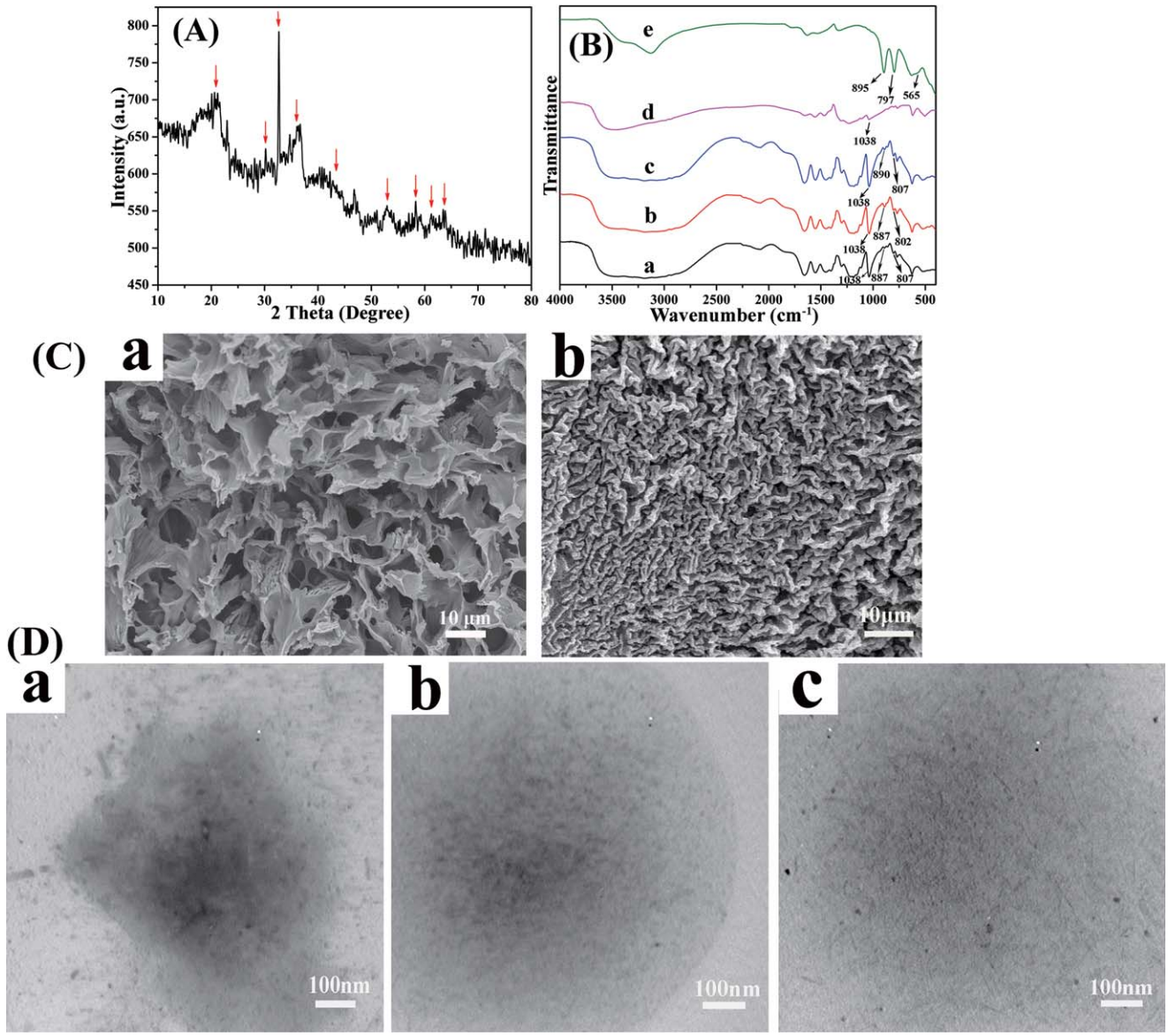

Figure 2. The structural characterization of PAMPS/Fe_3O_4 nanozyme. (A) X-ray diffractograms. (B) The FTIR spectra of PAMPS/Fe_3O_4 nanozymes with different crosslinking concentrations (a) 0.5 wt %; (b) 1.0 wt %; (c) 1.5 wt %; (d) PAMPS hydrogel with a crosslinking concentration of 1.0 wt %; and (e) pure Fe_3O_4 nanozyme. (C) The SEM images of (a) dry pure PAMPS hydrogel and (b) PAMPS/Fe_3O_4 nanozyme immersed in buffer solution before reaction. (D) The TEM images of the PAMPS/Fe_3O_4 nanozyme with different concentrations of the crosslinking agent (a) 0.5 wt %, (b) 1 wt %, (c) 1.5 wt %. [Color figure can be viewed in the online issue, which is available at wileyonlinelibrary.com.]

solution were varied (0.005, 0.0098, 0.098, 0.3, and 0.5 mmol L^{-1}, respectively) while TMB was fixed at a concentration of 0.55 mmol L^{-1}. The reaction was monitored at 652 nm by UV–vis spectra measurements. The initial oxidation rates (V) can be calculated by detecting the absorbance increase with time at 652 nm. Michaelis constant (K_m) was acquired by varying concentrations of TMB and H_2O_2. Catalytic parameters were calculated by fitting the absorbance data to the Michaelis-Menten eq. (2).

$$V = \frac{V\,max \cdot [S]}{Km + [S]} \quad (2)$$

The Michaelis–Menten equation describes the relationship between the rates of substrate conversion by an enzyme and the concentration of the substrate. In this equation, V and V_{max} is the rate and maximum rate of conversion, respectively; S is the substrate concentration and K_m is the Michaelis constant, which approximates the affinity of the enzyme for the substrate.

RESULTS AND DISUSSION

Synthesis and Characterization of the Hydrogel-Supported Fe_3O_4 Nanozyme

In situ synthesis of Fe_3O_4 nanozyme was carried out within PAMPS hydrogel networks as depicted in Figure 1. Translucent orange hydrogels loading ferrous (Fe^{2+}) and ferric ions (Fe^{3+}) were acquired by immersing PAMPS hydrogel [Figure 1(a)] into an aqueous solution of iron ions until adsorption equilibrium was reached [Figure 1(b)]. Finally, black opaque hydrogel-

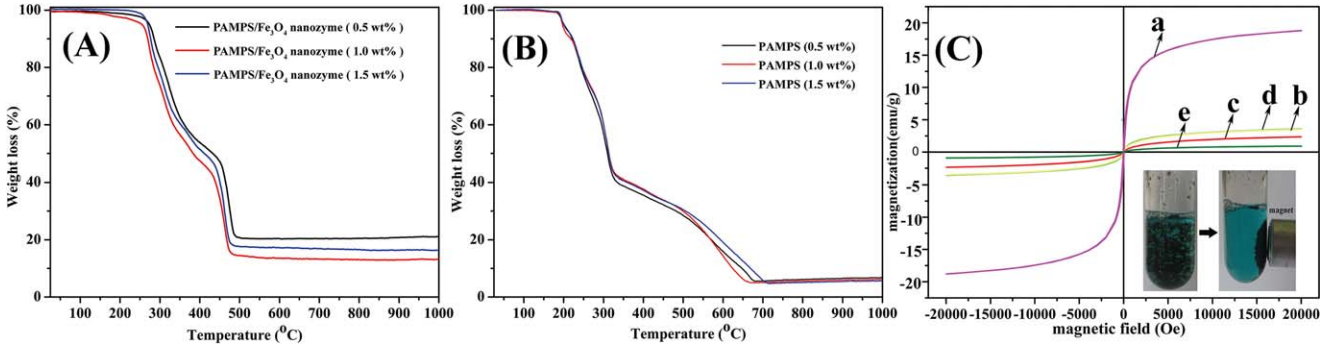

Figure 3. Thermograms of (A) hydrogel-supported Fe_3O_4 nanozyme and (B) pure hydrogel with different concentrations of the crosslinking agent (1.5, 1.0, and 0.5 wt % respectively). (C) Magnetization curve of (a) pure Fe_3O_4 nanozyme, PAMPS/Fe_3O_4 nanozyme with different crosslinking concentration (b) 1.5 wt %; (c) 1.0 wt %; (d) 0.5 wt %, (e) PAMPS/Fe_3O_4 nanozyme with a crosslinking concentration of 1.0 wt % after reaction. Inset: image of reaction solution before and after magnetic separation of PAMPS/Fe_3O_4 nanozyme. [Color figure can be viewed in the online issue, which is available at wileyonlinelibrary.com.]

supported Fe_3O_4 nanozyme was obtained after ammonia treatment [Figure 1(c)]. Different from the previous report,[23] in our present experiment, AMPS was used for polymerization without neutralization. It was expected to decrease the combination speed between the PAMPS hydrogel and iron ions due to weakened electrostatic interaction. As a result, Fe_3O_4 dispersion would be improved. Also aqueous ammonia treatment was carried out to obtain Fe_3O_4 nanozyme, which avoided the tediousness in the following Fe_3O_4 loading analysis caused by sodium hydroxide treatment.

The XRD patterns of the PAMPS/Fe_3O_4 nanozyme with 1 wt % of crosslinking concentration were checked in order to verify iron oxide phase [Figure 2(A)]. The peak positions located at 2 θ angles of 21.06, 30.27, 32.7, 35.96, 43.01, 52.9, 58.3, 61.27, and 63.51° demonstrated that the particles were Fe_3O_4 nanozyme with an inverse spinal structure.[26,27] The reason of peak broadening was given rise to the presence of ultrafine Fe_3O_4 nanozyme particles.

The chemical structure of PAMPS/Fe_3O_4 nanozyme was confirmed by FTIR spectra in Figure 2(B). The spectrum of pure Fe_3O_4 exhibited an absorption peak at 3129 cm^{-1}, which was the characteristic peak of –OH stretching vibration, suggesting the presence of ferric hydroxide in Fe_3O_4.[28] Meanwhile, the bands observed at 895 cm^{-1}, and 797 cm^{-1} can be attributed to the Fe–OH bending vibration, which was likely to result from the Fe_3O_4 nanozyme surface and the α-FeOOH. In addition, there was one absorption peak at 565 cm^{-1} was due to the vibrations of Fe^{2+} – O^{2-}, which was agreed with the reported IR spectra for spinel Fe_3O_4.[29] Above all, there was no 556 cm^{-1} or 478 cm^{-1} peak in the spectrum, which belonged to characteristic absorption peaks of iron oxide (Fe_2O_3). The result also confirmed that the materials contained crystallized Fe_3O_4 nanozyme. For the spectrum of hydrogel-supported Fe_3O_4 nanozyme, the broad band between 3500 cm^{-1} and 3200 cm^{-1} corresponded to N–H stretching from the amide groups in AMPS units and the cross-linker MBA, and overlapped O–H stretching from the sulfonic acid group in AMPS. The peak at 1656 cm^{-1} was attributed to carbonyl stretching in amide groups of PAMPS/Fe_3O_4 nanozyme. The N–H deformation vibration and N–H bending vibration were indicated by the bands observed at 1552 cm^{-1} and 1300 cm^{-1}, respectively. The peak at 1404 cm^{-1} corresponded to C–N stretching of an amide III band. The SO_3 symmetric stretching occurred at 1038 cm^{-1}. In contrast, the Fe–OH bending peak at near 890 cm^{-1} and 807 cm^{-1} were weaker than the peak of pure Fe_3O_4, which suggested that the PAMPS hydrogel can restrain the formation of α-FeOOH and promoted the growth of Fe_3O_4 crystalline grain. However, the peak at 565 cm^{-1} did not appear obviously in PAMPS/Fe_3O_4, which was likely to be overlapped by the PAMPS units. However, it can be concluded that the Fe_3O_4 nanozyme really existed in PAMPS hydrogel network, combined with TEM and XRD of PAMPS/Fe_3O_4 nanozyme. Moreover, there was no olefinic band ($v_{c=c}$) at 1635–1620 cm^{-1}, verifying the formation of the hydrogel thoroughly.

When PAMPS/Fe_3O_4 nanozyme was immersed in buffer solution before reaction, it swelled but in a low degree due to increased osmotic pressure compared with in deionized water. But in contrast to the pure PAMPS hydrogel {Figure 2[C(a)]}, PAMPS/Fe_3O_4 nanozyme showed lower swelling. As a result, network size of PAMPS/Fe_3O_4 nanozyme was small {Figure 2[C(b)]}. TEM images [Figure 2(D)] revealed that Fe_3O_4 nanozyme appeared to be uniformly dispersed in hydrogel network, which prevented efficaciously Fe_3O_4 nanozyme from aggregation. The presence of the hydrogel network improved the surface area of Fe_3O_4 nanozyme and would further increase the catalytic activity of the nanozyme. By relating the phase analysis result, it can be concluded that the particles observed by TEM were Fe_3O_4, while a bit of needlelike particles were α-FeOOH.[26] Moreover, more α-FeOOH was observed when the crosslinking concentration increased up to 1.5 wt %. This was caused by dehydration of excessive $Fe(OH)_3$ due to fast oxidation of Fe^{2+} into Fe^{3+}.[30] With the increasing crosslinking density, the phase transition became more obvious [Figure 2(D)].

In order to obtain the Fe_3O_4 nanozyme amount within the hydrogel, the magnetic nanocomposites and the pure hydrogel were analyzed by TGA in a nitrogen atmosphere, and their corresponding thermograms were displayed in Figure 3(A). The PAMPS/Fe_3O_4 nanozyme with different concentrations of the

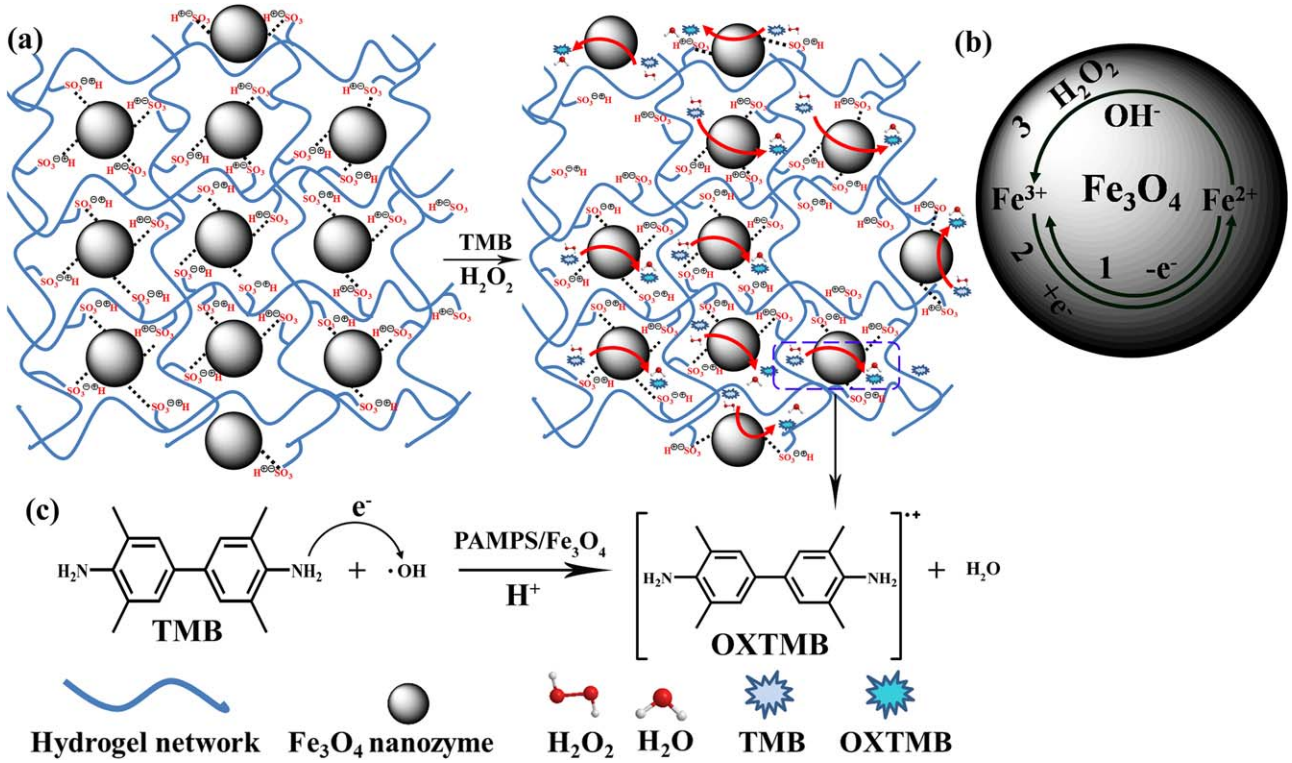

Figure 4. (a) A schematic of the catalytic activity based on Fe_3O_4 nanozyme within hydrogel network. (b) A proposed mechanism of the catalytic oxidation of H_2O_2 on Fe_3O_4 nanozyme catalysts within hydrogel matrices. (c) The reaction principles in TMB–H_2O_2 system. [Color figure can be viewed in the online issue, which is available at wileyonlinelibrary.com.]

crosslinking agent (1.5, 1.0, and 0.5 wt %, respectively) started to decompose at 276, 274, and 285°C, respectively, and ending decomposition temperatures were 482, 484, and 499°C, respectively, correspondingly initial decomposition temperatures of bare PAMPS hydrogels were 195, 194, and 194°C, respectively, and the final decomposition temperature were 709, 667, and 677°C, respectively [Figure 3(B)]. The contents of Fe_3O_4 nanozyme in the hydrogels with different concentrations of the crosslinking agent (1.5, 1.0, and 0.5 wt %) were calculated as 14.38 wt %, 10.91 wt %, and 16.45 wt %, respectively. So it can

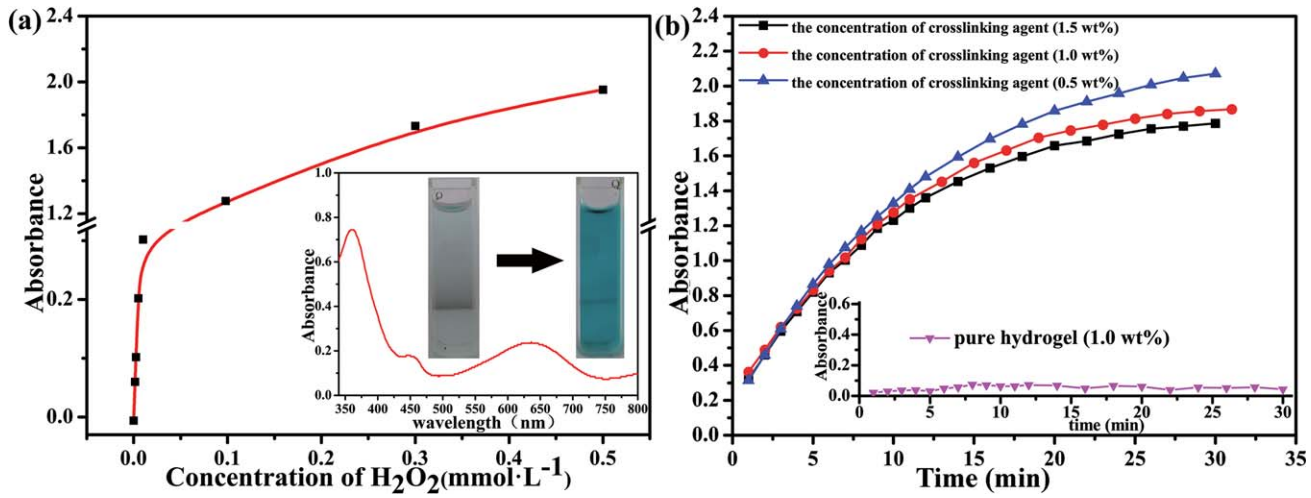

Figure 5. (a) A H_2O_2 concentration-response curve using the PAMPS/Fe_3O_4 nanozyme as a catalyst under the same reaction conditions and with a H_2O_2 concentration range of 1.5 μM to 0.5 mM. (b) UV–vis absorption-time course curves for PAMPS/Fe_3O_4 nanozymes with different concentration crosslinking agent (1.5, 1.0, and 0.5 wt % respectively) and pure PAMPS hydrogel (1.0 wt %) in the same buffer with TMB–H_2O_2. [Color figure can be viewed in the online issue, which is available at wileyonlinelibrary.com.]

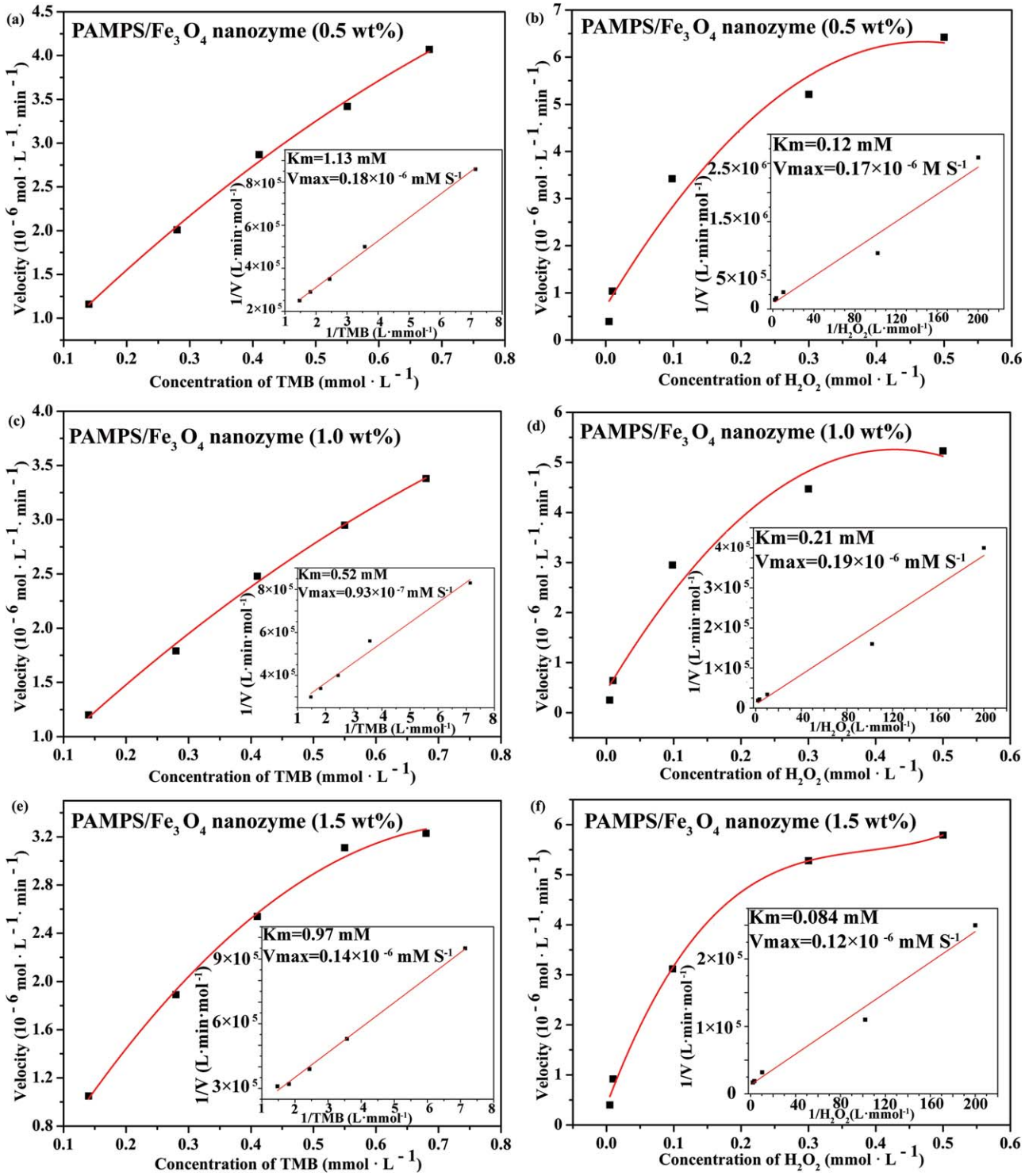

Figure 6. The reaction rate of hydrogel-supported Fe_3O_4 nanozyme in TMB–H_2O_2 reaction system with different concentrations of TMB and H_2O_2, the insert image is the double-reciprocal plots of activity of PAMPS/Fe_3O_4 nanozyme. [Color figure can be viewed in the online issue, which is available at wileyonlinelibrary.com.]

be found that the Fe_3O_4 loading did not increase monotonically with the decreasing of crosslinking concentration as expected. This indicated, besides of network size, the distribution of sulfonate groups was also a deciding factor on Fe_3O_4 loading. However, even if in different loading, the Fe_3O_4 nanozymes were all well dispersed in the PAMPS hydrogels, which would benefit the catalytic activity.

The magnetic property of the prepared composites with different crosslinking concentration was recorded with a vibrating

Table I. Apparent Kinetic Parameters for the Hydrogel-Supported Fe_3O_4 Nanozyme with Different Concentrations of the Crosslinking Agent (1.5 wt %, 1 wt %, and 0.5 wt %) to the TMB and H_2O_2

	Substrate	K_m/m*M*	V_{max}/m*M* S^{-1}
PAMPS/Fe_3O_4 (0.5 wt %)	TMB	1.13	1.8×10^{-7}
	H_2O_2	0.12	1.7×10^{-7}
PAMPS/Fe_3O_4 (1.0 wt %)	TMB	0.52	9.3×10^{-8}
	H_2O_2	0.21	1.9×10^{-7}
PAMPS/Fe_3O_4 (1.5 wt %)	TMB	0.97	1.4×10^{-7}
	H_2O_2	0.084	1.2×10^{-7}

K_m is the Michaelis constant, and V_{max} is the maximal reaction velocity.

sample magnetometer. Figure 3(C) showed that the magnetization hysteresis loop of the PAMPS/Fe_3O_4 nanozyme in the applied magnetic field from −20 to 20 kOe at room temperature and demonstrated that the composite had a ferromagnetic property. The saturation magnetization of PAMPS/Fe_3O_4 nanozyme (1.5, 1, 0.5 wt %) were 3.60, 2.36, and 3.57 emu/g, respectively, which were smaller than those of Fe_3O_4 nanozyme (18.8 emu/g). The magnetism had a close relationship with the loading. The reduced value might be attributed to the existence of diamagnetic contribution from the PAMPS hydrogel matrix on the surface of Fe_3O_4 nanozyme and the spin canting of surface Fe atoms.[31] Cai *et al.* reported 1.66 emu/g of low-saturation magnetization when the Fe_3O_4 content was 6.33 wt % due to diamagnetic contribution of the SiO_2 shells coated the Fe_3O_4 nanozyme.[32] The saturation magnetization of the hydrogel-supported Fe_3O_4 nanozyme (1 wt %) after reaction was 0.91 emu/g. It was possible reason of the phenomenon that the leaching of iron from magnetic nanoparticles into aqueous solution during reaction process or partial oxidation of Fe_3O_4 nanozyme.[15] The phenomenon of iron leaching can be explained in the following two reasons: (i) Under acidic condition, Fe_3O_4 nanozyme would release a small amount Fe ions.[33] (ii) The combination of Fe_3O_4 nanozyme with the hydrogel might be partly broken in the presence of reactants and products [Figure 4(b)]. But, it was sufficient for catalyst separation from solution with an external magnet, as shown in the inset of Figure 3(C).

Peroxidase-Like Activity and H_2O_2 Detection

In order to investigate the intrinsic peroxidase-like activity of the PAMPS/Fe_3O_4 nanozyme, the catalytic oxidation of peroxidase substrate TMB as a chromogenic substrate in the presence of H_2O_2 was carried out at room temperature. In addition, the absorbance of the TMB oxidation product was recorded with UV–vis at 652 nm. The result demonstrated that the intrinsic peroxidase-like activity of the Fe_3O_4 nanozyme can still be preserved after *in situ* formation within a hydrogel network. The schematic of the catalytic performance based on hydrogel-supported Fe_3O_4 nanozyme was shown in Figure 4(a). The peroxidase-like activity originated mainly from the interconversion among ferrous ions at the surface of Fe_3O_4 nanozyme [Figure 4(b)] and Figure 4(c) showed the reaction principles in TMB–H_2O_2 system. The nanozyme was loaded within the hydrogel matrices presenting the high catalytic activity in our system, and it was chosen for the H_2O_2 detection at different concentrations (1.5 μM−0.5 m*M*). The result indicated that the catalytic activity increased with an increase in H_2O_2 concentration, and the H_2O_2 can be detected even at a concentration as low as 1.5×10^{-6} mol L^{-1}, which was three times lower than the one in the case of PNaAMPS hydrogel-supported Fe_3O_4 nanoparticles.[23] The linear detection range is 1.5–9.8 μM [Figure 5(a)]. Meanwhile, different reaction systems were catalyzed by the PAMPS/Fe_3O_4 nanozyme with different crosslinking concentration (1.5, 1.0, and 0.5 wt %, respectively) within 30 min, and the time course curves were shown in Figure 5(b). And in order to clarify whether pure PAMPS hydrogel affected the reaction, we evaluated the influence of pure PAMPS hydrogel (1.0 wt %) on the catalytic activity. We found that pure PAMPS hydrogel (1.0 wt %) hardly affected the reaction [Figure 5(b)]. The PAMPS/Fe_3O_4 nanozyme showed high catalytic efficiency but in different levels of activity towards TMB in the order with the different crosslinking concentrations: 0.5 wt % > 1.0 wt % > 1.5 wt %. In general, the high catalytic efficiency of PAMPS/Fe_3O_4 nanozyme can be mainly attributed to the high dispersion of Fe_3O_4 nanozyme within hydrogel network. The superior catalytic performance of PAMPS hydrogel-supported Fe_3O_4 nanozyme can be explained in the following two ways: (i) PAMPS hydrogel can prevent particle–particle aggregation, providing high effective surface area, and (ii) the electron-donating sulfur group of the polymer (PAMPS) can suppress leaching of iron through coordination formation to some extent, facilitating the catalytic reaction in the confined region of the nanoparticle surface.[34] It seemed not to be proportional to the contents of Fe_3O_4 nanozyme in our experimental condition. More impurity may lead to a decrease in catalytic efficiency in some degree though a high loading of 16.45 wt % was found in the hydrogel with a crosslinking concentration of 1.5 wt %. Besides, network size of the hydrogel acted an important role in catalytic efficiency since it could affect the substrate transfer process. It will be helpful for reactants to diffuse into the hydrogel with a larger network produced by lower crosslinking concentration. This further exhibited that the hydrogel was not only as a carrier but also can provide a specific microenvironment for the catalytic reaction. When there was no big difference on the content of Fe_3O_4 nanozyme, the lower crosslinking concentration lead to the higher catalytic activity of the PAMPS/Fe_3O_4 nanozyme. As a result, we can adjust the crosslinking concentrations to improve the catalytic activity of hydrogel-supported nanozyme.

The Steady-State Kinetics

The apparent steady-state kinetic parameters for the reaction with PAMPS/Fe_3O_4 nanozyme as a catalyst were then determined at room temperature. Absorbance data were back-calculated to concentration by the Beer-Lambert Law and a molar absorption coefficient of 39,000 L mol^{-1} cm^{-1} for TMB-derived oxidation product was used for the calculation.[35] We observed that the catalytic oxidation reaction performed by the PAMPS/Fe_3O_4 nanozyme followed a Michaelis-Menten behavior towards the TMB and H_2O_2 and the corresponding 1/V-1/S curve were shown in Figure 6. The initial oxidation rates (V) at different concentrations of substrate were acquired by calculating the slopes of absorbance increases with time at 652 nm. The catalytic parameters were calculated by fitting the absorbance data to the Michaelis-Menten equation, as shown in Table I. The K_m value of the PAMPS/Fe_3O_4 nanozyme (1 wt %) with TMB as the substrate was a bit lower than for PAMPS/Fe_3O_4 nanozyme (0.5 wt %) and PAMPS/Fe_3O_4 nanozyme (1.5 wt %), implying that the PAMPS/Fe_3O_4 nanozyme (1 wt %) had a higher affinity towards TMB than the other two. This phenomenon was caused by different dispersion: the dispersion Fe_3O_4 nanozyme within the PAMPS hydrogel (1.0 wt %) network was better than the other two, which can be revealed by the TEM [Figure 2(D)]. But the K_m value of PAMPS/Fe_3O_4 nanozyme (1 wt %) with H_2O_2 as the substrate was significantly higher than the other two, suggesting that a higher concentration of H_2O_2 was required to obtain maximal reaction velocity for PAMPS/Fe_3O_4 nanozyme (1 wt %). In contrast, the K_m value for TMB was higher than that for H_2O_2, which was possibly caused by the differences on hydrophilicity and size between TMB and H_2O_2. TMB with amine groups yielded strong affinity with negatively charged Fe_3O_4 nanoparticles. Lower loading of Fe_3O_4 nanozyme resulted in higher affinity towards TMB. However, the affinity between H_2O_2 and PAMPS/Fe_3O_4 nanozyme was not driven by electrostatic attraction but polar interaction. As a result, affinity towards H_2O_2 was not only decided on dispersion and contents of Fe_3O_4 nanozyme, but also on the network structure of the hydrogel. In fact, the reaction velocity was obviously reduced due to shielding effect of hydrogel network compared with other modifiers.

CONCLUSIONS

In summary, the hydrogel-supported Fe_3O_4 nanozyme were synthesized by *in situ* synthesis of Fe_3O_4 nanozyme in PAMPS hydrogel network and characterized by TEM, FTIR, UV–vis, TG, XRD, SEM, and VSM. The PAMPS/Fe_3O_4 nanozyme not only reserved magnetism but also presented intrinsic peroxidase-like activity and exhibited a high catalytic activity. The crosslinking concentration of PAMPS hydrogel made an important effect in the catalytic activity in our experimental condition. The lower crosslinking concentration leaded to the higher catalytic activity of the PAMPS/Fe_3O_4 nanozyme. In addition, the hydrogel-supported Fe_3O_4 nanozyme had a sensitive response towards H_2O_2 detection with a limit of 1.5×10^{-6} mol L^{-1} with a linear range of 1.5–9.8 $\times$ 10^{-6} mol L^{-1}. The affinity between the hydrogel-supported Fe_3O_4 nanozyme and substrates can be improved by adjusting the crosslinking concentration of the PAMPS hydrogel without other trenchant experimental conditions. As nanoparticle enzyme mimetics, the catalysis of PAMPS/Fe_3O_4 nanozyme showed typical Michaelis-Menten kinetics. Such investigations not only guided us to enhance catalytic efficiency of hydrogel-supported Fe_3O_4 nanozyme by alteration of crosslinking concentration of hydrogel, but also showed potential applications in bio-detection and environmental chemistry.

ACKNOWLEDGMENTS

This work was kindly supported by the Natural Science Foundation of China (No. 21366031) and NSFC-Xinjiang joint fund for local outstanding youth (No. U1403392).

REFERENCES

1. Xie, J.; Zhang, X.; Wang, H.; Zheng, H.; Huang, Y.; Xie, J. *TrAC, Trends Anal. Chem.* **2012**, 114.
2. Gross, M. *Curr. Biol.* **2013**, *23*, 214.
3. Dutton, P. L.; Moser, C. C. *Faraday Discuss.* **2011**, *148*, 443.
4. Quin, M. B.; Schmidt-Dannert, C. *ACS Catal.* **2011**, *1*, 1017.
5. Mateo, C.; Palomo, J. M.; Fernandez-Lorente, G.; Guisan, J. M.; Fernandez-Lafuente, R. *Enzyme Microb. Technol.* **2007**, *40*, 1451.
6. Nanda, V.; Koder, R. L. *Nat. Chem.* **2010**, *2*, 15.
7. Pryor, S. W.; Nahar, N. *Appl. Biochem. Biotechnol.* **2010**, *162*, 1737.
8. Miletic, N.; Nastasovic, A.; Loos, K. *Bioresour. Technol.* **2012**, *115*, 126.
9. Gao, L.; Zhuang, J.; Nie, L.; Zhang, J.; Zhang, Y.; Gu, N.; Wang, T.; Feng, J.; Yang, D.; Perrett, S.; Yan, X. *Nat. Nanotechnol.* **2007**, *2*, 577.
10. Wei, H.; Wang, E. *Chem. A Anal. Chem.* **2008**, *80*, 2250.
11. Yu, F.; Huang, Y.; Cole, A. J.; Yang, V. C. *Biomaterials* **2009**, *30*, 4716.
12. Arana, M.; Tettamanti, C. S.; Bercoff, P. G.; Rodríguez, M. C. *Electroanalysis* **2014**, *26*, 1721.
13. Dong, Y. L.; Zhang, H. G.; Rahman, Z. U.; Su, L.; Chen, X. J.; Hu, J.; Chen, X. G. *Nanoscale* **2012**, *4*, 3969.
14. Zhang, J.; Zhuang, J.; Gao, L.; Zhang, Y.; Gu, N.; Feng, J.; Yang, D.; Zhu, J.; Yan, X. *Chemosphere* **2008**, *73*, 1524.
15. Zhang, S.; Zhao, X.; Niu, H.; Shi, Y.; Cai, Y.; Jiang, G. *J. Hazard. Mater.* **2009**, *167*, 560.
16. Chen, J.; Liu, Y.; Zhu, G.; Yuan, A. *Cryst. Res. Technol.* **2014**, *49*, 309.
17. Ye, X. Y.; Liu, Z. M.; Wang, Z. G.; Huang, X. J.; Xu, Z. K. *Mater. Lett.* **2009**, *63*, 1810.
18. Nath, S.; Kaittanis, C.; Ramachandran, V.; Dalal, N. S.; Perez, J. M. *Chem. Mater.* **2009**, *21*, 1761.
19. Zeng, T.; Bai, Y.; Li, H.; Yao, W. F. *Nano* **2015**, *10*, 1550063.
20. Zhang, X. Q.; Gong, S. W.; Zhang, Y.; Yang, T.; Wang, C. Y.; Gu, N. *J. Mater. Chem.* **2010**, *20*, 5110.
21. Murali Mohan, Y.; Lee, K.; Premkumar, T.; Geckeler, K. E. *Polymer* **2007**, *48*, 158.

22. Sivudu, K. S.; Reddy, N. M.; Prasad, M. N.; Raju, K. M.; Mohan, Y. M.; Yadav, J. S.; Sabitha, G.; Shailaja, D. *J. Mol. Catal. A Chem.* **2008**, *295*, 10.

23. Gao, Y.; Wei, Z.; Li, F.; Yang, Z. M.; Chen, Y. M.; Zrinyi, M.; Osada, Y. *Green Chem.* **2014**, *16*, 1255.

24. Noguchi, H.; Yanase, N.; Uchida, Y.; Suzuta, T. *J. Appl. Polym. Sci.* **1993**, *48*, 1539.

25. Peniche, H.; Osorio, A.; Acosta, N.; de la Campa, A.; Peniche, C. *J. Appl. Polym. Sci.* **2005**, *98*, 651.

26. Zhou, Z. H.; Wang, J.; Liu, X.; Chan, H. S. O. *J. Mater. Chem.* **2001**, *11*, 1704.

27. Si, S.; Kotal, A.; Mandal, T. K.; Giri, S.; Nakamura, H.; Kohara, T. *Chem. Mater.* **2004**, *16*, 3489.

28. Ahmad, S.; Riaz, U.; Kaushik, A.; Alam, J. *J. Inorg. Organmet. Polym.* **2009**, *19*, 355.

29. Meng, J.; Yang, G.; Yan, L.; Wang, X. *Dyes Pigments* **2005**, *66*, 109.

30. Jia, B.; Gao, L. *J. Am. Ceram. Soc.* **2006**, *89*, 1739.

31. Saravanan, P.; Alam, S.; Mathur, G. *J. Mater. Sci. Lett.* **2003**, *22*, 1283.

32. Cai, J.; Guo, J.; Ji, M.; Yang, W.; Wang, C.; Fu, S. *Colloid. Polym. Sci.* **2007**, *285*, 1607.

33. Shin, S.; Yoon, H.; Jang, J. *Catal. Commun.* **2008**, *10*, 178.

34. Shin, S.; Jang, J. *Chem. Commun.* **2007**, *41*, 4230.

35. Karaseva, E.; Losev, Y. P.; Metelitsa, D. *Russ. J. Bioorganic Chem.* **2002**, *28*, 128.